A spectral-based method for tissue characterization

Janusz WÓJCIK, Michał BYRA, Andrzej NOWICKI

Ultrasound Department,
Institute of Fundamental Technological Research,
Polish Academy of Sciences
Pawińskiego 5B, Warsaw, Poland
mbyra@ippt.pan.pl

Quantitative ultrasound methods are widely investigated as a promising tool for tissue characterization. In this paper, a novel quantitative method is developed which can be used to assess scattering properties of tissues. The proposed method is based on analysis of oscillations of the backscattered echo power spectrum. It is shown that these oscillations of the power spectrum are connected with the distances between scatterers within the medium. Two techniques are proposed to assess the scatterer's distribution. First, we show that the inverse Fourier transform of the backscattered echo power spectrum corresponds to a histogram of the distances between scatterers. Second, the Hilbert-Huang transform is used to directly extract the power spectrum oscillations. Both methods are examined by means of a numerical experiment. A cellular gas model of a biological medium is considered. Results are presented and discussed. Both methods can be used to evaluate the scatterer's distribution by means of the power spectrum oscillations.

Keywords: quantitative ultrasound, signal analysis, wave scattering.

1. Introduction

Quantitative ultrasound (QUS) methods are now widely investigated as a promising tool for tissue characterization [1, 2], temperature monitoring [3] or breast lesion diagnosis [4]. In comparison to standard ultrasound imaging, based on reflectivity, QUS techniques assess different tissue properties. These methods can be used to create B-mode like parametric maps [5–9] A great number of QUS methods are spectral-based. The backscattered echo spectrum carries information about scattering properties within the investigated tissue. For instance, the spectrum of backscattered ultrasound can be used to calculate the attenuation [10], nonlinearity parameter [11] or assess tissue stiffness [12]. QUS methods are usually based on physical models of the medium; however, there are efforts to model the spectrum as a time-

series, and extract useful features for tissue characterization [13,14]. While the spectrum of the ultrasonic pulse reflected from a single scatterer is similar to the spectrum of the transmitted pulse, the signal resulting from reflection on a cluster of scatterers is much more complex; the spectrum becomes less smooth, exhibiting strong variability reflecting local, specific, scattering conditions in the tissue.

In this paper, a novel spectral-based method for tissue characterization is described. Our method is based on analysis of the backscattered echo spectrum. It is proved that the spectrum variability can be used for tissue characterization. First, a model is derived to show that the spectrum variability is related to the scatterers' distribution. For this purpose, the model of point scatterers is used. The backscattered echo power spectrum can be split into the spectrum of the emitted signal, and a part characterizing the medium. Next, the Hilbert-Huang transform (HHT) is applied to decompose the power spectrum into so-called "intrinsic mode functions" (IMF). It is depicted that IMFs caries information on the spectrum variability.

2. Materials and methods

In this study, a 1-D model of the medium, consisting of point scatterers will be considered. Let us express the scattering from a point target as:

$$f(t) = wp(t - t_i), \tag{1}$$

where w is the reflectivity of the point scatterer. It describes the physical properties of the scatterer, and the capacity to reflect the incident ultrasound pulse $p(t)$. It must be stated that in our model the incident wave is not modified as it propagates through the medium. The time shift t_i corresponds to the scatterer's position by means of the relation $t_i = \frac{2z_i}{c}$, where z_i is the propagation distance and c is the speed of sound (constant speed of sound c is assumed).

Let us consider the medium consisting of J scatterers. The spectrum of backscattered echo from a collection of J scatterers can be expressed as a linear combination:

$$E(\omega) = P(\omega)H(\omega) = P(\omega)\sum_{j}^{J} w_j\, e^{-i\omega t_j}, \tag{2}$$

where $P(\omega)$ is the Fourier transform of the emitted pulse, the sum $H(\omega)$ characterizes the medium, w_j and t_j are the reflectivity and time (spatial) shift of the j-th scatterer, respectively. Additionally, the power spectrum is given by:

$$Q_E(\omega) = E(\omega)E^*(\omega) = |P(\omega)|^2 \sum_{j}^{J} w_j\, e^{-i\omega t_j} \sum_{h}^{J} w_h\, e^{i\omega t_h} =$$

$$= |P(\omega)|^2 \left\{ \sum_{j} w_j^2 + \sum_{j,h:j<h} 2w_j w_h \cos(\omega(t_h - t_j)) \,. \right\}. \tag{3}$$

The power spectrum $Q_E(\omega)$ is the Fourier transform of the autocorrelation function. According to the eq.(3), the power spectrum is a product of the emitted pulse power spectrum and an oscillatory part describing spectrum variability. The last part is connected with the distances between scatterers $t_h - t_j = \frac{2(z_h - z_j)}{c} = \frac{2d_{h,j}}{c}$ in the medium.

In order to estimate the spatial distribution of distances $q(d)$ (histogram) between scatterers, the inverse Fourier transform of the oscillatory part in eq. (3) must be calculated:

$$q'(t) = F^{-1}\left\{\sum_j w_j^2 + \sum_{j,h:j<h} 2w_j w_h \cos(2\frac{\omega}{c} d_{h,j})\right\} =$$

$$= \sum_j w_j^2 \delta(0) + \sum_{j,h:j<h} 2w_j w_h \delta(t - \frac{2d_{h,j}}{c}) =$$

$$= q(d) = \sum_j w_j^2 \delta(0) + \sum_{j,h:j<h} c w_j w_h \delta(d - d_{h,j}), \quad (4)$$

where $\delta(\cdot)$ is the Dirac delta function and $t = \frac{2d}{c}$. The above sum can be interpreted as a histogram of distances between scatterers with reflectivities $w_j w_h$ that measure the importance of a particular distance d_{hj}. Generally, for J scatterers there will be $J(J\text{-}1)/2$ possible distances. With equidistant scatterers, the shape of the histogram can be easily predicted. However, to model biological conditions, scatterers must be localized randomly. To accomplish this, a cellular automaton discrete model was utilized. The line of length L was divided into J equal bins (one for each scatterer) of length $D=L/J$. The position of the j-th scatterers was given by $z_j = z_{oj} + \varsigma_j$, $z_{oj} = (j - 1/2)D$ was the position of the j-th bin's center. The random variable ς_j was used to provide a random position of the scatterer in the cell. In our study, ς_j was sampled from the uniform distribution on the interval $\left[-\frac{\chi D}{2}, \frac{\chi D}{2}\right]$, where $0 < \chi < 1$ is the level of chaotization, when scatterers are placed regularly $\chi = 0$.

Equation (3) suggests that the oscillations of the power spectrum are related to the scatterer's spatial distribution, and that these oscillations are modified by the power spectrum of the emitted pulse (multiplicative process). The band-width of the emitted pulse is crucial, since the use of a wide-band pulse would result in illegibility of the histogram in eq. (4). This raises the question of how to measure the oscillations efficiently, since the histogram may be biased. To address this issue and extract the oscillations, the HHT method was used [15]. The HHT algorithm allows you to decompose a signal into so-called IMF along with the trend. It works well for signals that are nonstationary and nonlinear. Each IMF carries information about the oscillations of the analyzed signal. In ultrasound imaging, usually Gaussian pulses (or similar) are used, which corresponds to spectrums that are Gaussian shaped. In our case, the HHT can be used to extract from eq. (4) the emitted pulse power spectrum (trend), and the oscillations as IMFs. To decompose the signal, the empirical mode decomposition (EMD) method is used:

1. Identify all the local extremes in the signal.
2. Connect all the local maxima to create the upper envelope
3. Connect all the local minima to create the lower envelope
4. Calculate the mean envelope
5. Subtract the mean envelope from the signal to obtain the first IMF.

Next, the analyzed signal is replaced by the first IMF and the EMD is repeated. Some kind of interpolation must be used to calculate envelopes; and, in our study, linear interpolation was applied. Linear interpolation proved to be robust. What is more, it doesn't generate artefacts, although it may be less suitable for the analysis of rapidly-changing signals. The HHT decomposition is linear, by summing of IMFs and trends it is possible to reconstruct the original signal.

3. Results

For the numerical simulation, L and J were set to 20 mm and 20, respectively. It corresponds to cells that are equidistant. In this case, regularly placed scatterers would be apart from each other by 1 mm. Additionally, reflectivities were sampled from the uniform distribution on the interval $[-0.5,\ 0.5]$. An exemplary realization is shown in the fig. 1.

First, different levels of chaotization were set, and the power spectrum of the medium (eq.3) was calculated. Results are depicted in the fig. 2. Additionally, the histograms of distances (eq.4) are presented. Here, the emitted pulse power spectrum was not considered; instead, a quasi-Dirac delta function was used for calculations. For clarity, the reflectivities were set to 1.

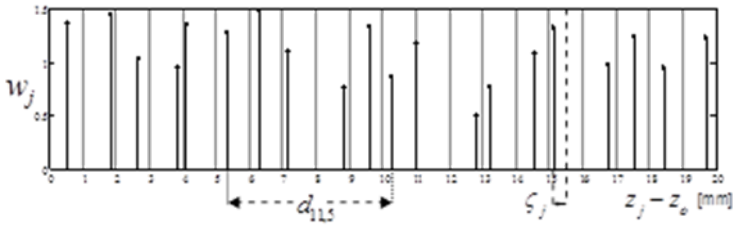

Fig. 1. Exemplary realization of the randomly allocated scatterers with different reflectivities.

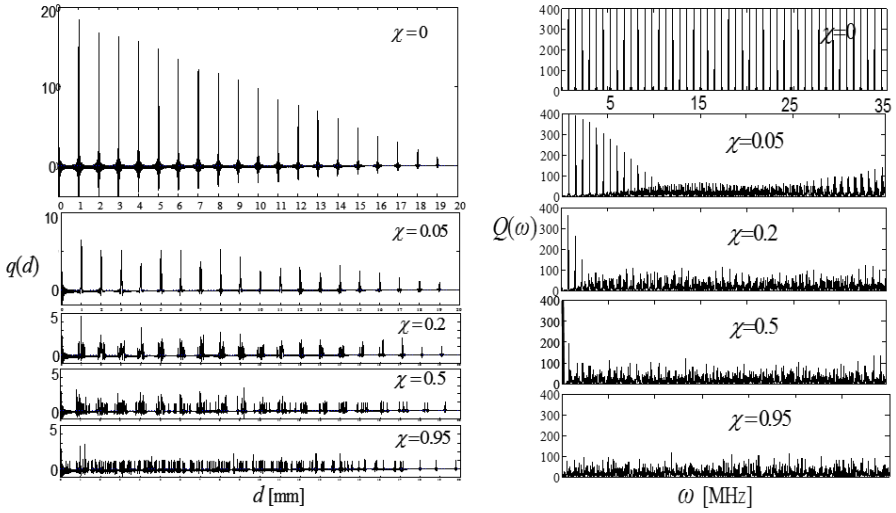

Fig. 2. Histogram of distances, and the power spectrum, for different levels of chaotization.

Next, the spectrum of emitted pulse was also considered. The center frequency was set to 5 MHz. Fig. 3 illustrates the HHT method. The power spectrum of the backscattered echo $Q(\omega)$ and four extracted IMFs are presented, along with the histograms. Due to the linearity of the Fourier transform, it is possible to reconstruct the original power spectrum or histogram.

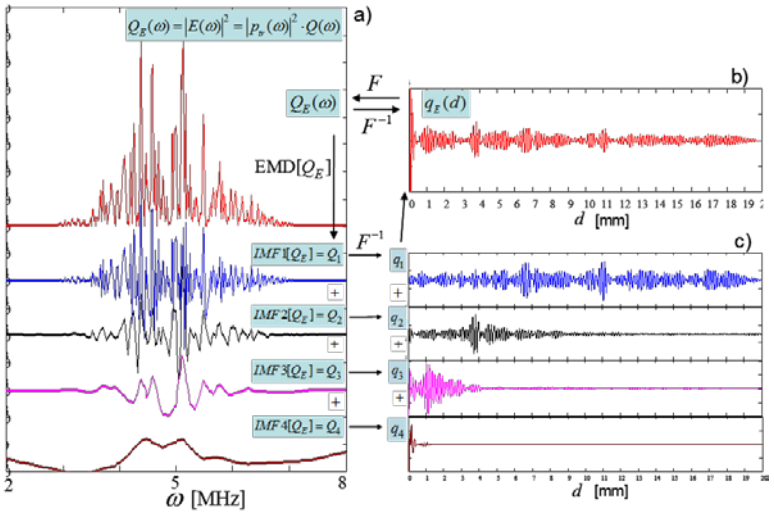

Fig. 3. The power spectrum of the backscattered echo and its IMFs, along with the histograms of distances (eq.4).

4. Discussion

As can be observed in fig. 2, the histogram can be simply used to calculate unique distances between scatterers. For example, for 20 equidistant scatterers there will be 19 distances of 1 mm. However, with the increased level of chaotization, the histogram becomes flatter, which corresponds to a larger number of unique distances between scatterers. What is important, therefore, when the chaotization level is low, the histogram is still able to perceive that the scatterers were placed in cells. This proves, that the derived method is sensitive to the coherent scattering which occurs when the scatterers are regularly distributed. However, in the case of backscattered echo, the power spectrum of the medium would be additionally multiplied by the spectrum of the emitted pulse. This multiplication in the frequency domain corresponds to a convolution which would blur the histogram, and make the exact calculation of distances impossible.

On the other hand, the HHT method can be used to extract oscillations directly from the power spectrum, which is illustrated in the fig. 3. The original power spectrum is depicted in red (top left image), its shape corresponds to the emitted pulse power spectrum that was affected by strong oscillations. Clearly, the IMFs extract oscillations. What is more, each subsequent IMF refers to oscillations of lower frequency. According to eq. (3), lower oscillations are caused by larger distances between scatterers. With the HHT method it is possible to extract oscillations which correspond to different distances between scatterers. However, it is hard to indicate which distances are included in a particular IMF. This reveals a disadvantage of the HHT algorithm. On the other hand, IMFs can be further analyzed with the Fourier transform, or other methods, to extract features that characterize the scatterer's distribution. For instance, each IMF caries unique information about distances of scatterers,

therefore its histogram (inverse Fourier transform) corresponds to these particular distances. After the HHT decomposition, it is possible to take the inverse Fourier transform of each IMF to obtain histograms as shown in the fig. 3. Due to linearity of the inverse Fourier transform, histograms can be summed up to reconstruct the original histogram. This proves that the HHT has the ability to decompose the histogram into parts which depend on different oscillations.

5. Conclusions

In this study, a novel QUS method was developed and examined by means of a numerical experiment. Point scatterers were randomly distributed, and different levels of chaotization were assumed. Oscillations of the backscattered echo power spectrum are caused by the distribution of scatterers. As it was derived, the function $q(d)$ can be interpreted as a histogram of distances. When the emitted pulse is not considered, the histogram can be simply used to calculate unique distances between scatterers. The HHT method can be applied directly to extract oscillations from the power spectrum. Each IMF corresponds to oscillations that were caused by different distances between scatterers. We believe that our two methods, the histogram of distances and HHT decomposition, can be used for tissue characterization. However, the proposed methods require experimental validation to evaluate their quality, and comparison with other widely used QUS methods.

Acknowledgments

This work was supported by National Science Center Grant Number UMO-2014/13/B/ST7/01271.

References

[1] J. Mamou, M.L. Oelze, Quantitative Ultrasound in Soft Tissues, Springer Netherlands, 2013.

[2] M.L. Oelze, J. Mamou, Review of Quantitative Ultrasound: Envelope Statistics and Backscatter Coefficient Imaging and Contributions to Diagnostic Ultrasound, IEEE Trans. Ultrason. Ferroelectr. Freq. Control. 63 (2016) 336–351.

[3] M. Byra, B. Gambin, Temperature detection based on nonparametric statistics of ultrasound echoes, Hydroacoustics. 18 (2015) 17–23.

[4] A. Nowicki, H. Piotrzkowska-Wroblewska, J. Litniewski, M. Byra, B. Gambin, E. Kruglenko, K. Dobruch-Sobczak, Differentiation of normal tissue and tissue lesions using statistical properties of backscattered ultrasound in breast, in: Ultrason. Symp. (IUS), 2015 IEEE Int., 2015: pp. 1–4.

[5] H. Tadayyon, A. Sadeghi-Naini, G.J. Czarnota, Non-invasive characterization of locally advanced breast cancer using textural analysis of quantitative ultrasound parametric images, Transl. Oncol. 7 (2014) 759–767.

[6] H. Tadayyon, A. Sadeghi-Naini, L. Wirtzfeld, F.C. Wright, G. Czarnota, Quantitative ultrasound characterization of locally advanced breast cancer by estimation of its scatterer properties., Med. Phys. 41 (2014) 12903.

[7] P.H. Tsui, C.K. Yeh, Y.Y. Liao, C.C. Chang, W.H. Kuo, K.J. Chang, C.N. Chen, Ultrasonic Nakagami Imaging: A Strategy to Visualize the Scatterer Properties of Benign and Malignant Breast Tumors, Ultrasound Med. Biol. 36 (2010) 209–217.

[8] M. Byra, A. Nowicki, H. Piotrzkowska-Wróblewska, K. Dobruch-Sobczak, Classification of breast lesions using segmented quantitative ultrasound maps of

homodyned K distribution parameters, Med. Phys. 43 (2016) 5561–5569.
[9] M. Byra, A. Nowicki, H. Piotrzkowska-Wroblewska, J. Litniewski, K. Dobruch-Sobczak, Correcting the influence of tissue attenuation on Nakagami distribution shape parameter estimation, in: Ultrason. Symp. (IUS), 2015 IEEE Int., 2015: pp. 1–4.
[10] F.L. Lizzi, E.J. Feleppa, S. Kaisar Alam, C.X. Deng, Ultrasonic spectrum analysis for tissue evaluation, Pattern Recognit. Lett. 24 (2003) 637–658.
[11] R. van Sloun, L. Demi, C. Shan, M. Mischi, Ultrasound coefficient of nonlinearity imaging, IEEE Trans. Ultrason. Ferroelectr. Freq. Control. 62 (2015) 1331–1341.
[12] A. Nowicki, M. Byra, J. Litniewski, J. Wójcik, Two frequencies push-pull differential imaging, in: 2014 IEEE Int. Ultrason. Symp., 2014: pp. 710–713.
[13] S. Granchi, E. Vannacci, E. Biagi, L. Masotti, Multidimensional spectral analysis of the ultrasonic radiofrequency signal for characterization of media, Ultrasonics. 68 (2016)
[14] N. Uniyal, H. Eskandari, P. Abolmaesumi, S. Sojoudi, P. Gordon, L. Warren, R.N. Rohling, S.E. Salcudean, M. Moradi, Ultrasound RF time series for classification of breast lesions, IEEE Trans. Med. Imaging. 34 (2015) 652–661.
[15] N.E. Huang, Z. Shen, S.R. Long, M.C. Wu, H.H. Shih, Q. Zheng, N.-C. Yen, C.C. Tung, H.H. Liu, The empirical mode decomposition and the Hilbert spectrum for nonlinear and non-stationary time series analysis, Proc. R. Soc. A Math. Phys. Eng. Sci. 454 (1998) 903–995.